8-9-2013

Aggregatibacter Actinomycetemcomitans Leukotoxin Utilizes a Cholesterol Recognition/Amino Acid Consensus Site for Membrane Association

Angela C. Brown
University of Pennsylvania

Angela C. Balashova
University of Pennsylvania

Richard M. Epand

Raquel F. Epand

Alvina Bragin

See next page for additional authors

Recommended Citation

Brown, A. C., Balashova, A. C., Epand, R. M., Epand, R. F., Bragin, A., Kachlany, S. C., Walters, M. J., Du, Y., Boesze-Battaglia, K., & Lally, E. T. (2013). Aggregatibacter Actinomycetemcomitans Leukotoxin Utilizes a Cholesterol Recognition/Amino Acid Consensus Site for Membrane Association. *Journal of Biological Chemistry, 288* (32), 23607-23621. http://dx.doi.org/10.1074/jbc.M113.486654

Aggregatibacter Actinomycetemcomitans Leukotoxin Utilizes a Cholesterol Recognition/Amino Acid Consensus Site for Membrane Association

Abstract

Background: A repeats-in-toxin (RTX) leukotoxin and its integrin receptor aggregate in cholesterol-rich lipid rafts. Results: The affinity of the toxin to cholesterol is driven by a cholesterol recognition/amino acid consensus (CRAC) motif. Conclusion: Leukotoxin cytotoxicity is regulated by the CRAC motif. Significance: Other RTX toxins contain this CRAC motif, suggesting a role for cholesterol recognition in RTX cytolysis. © 2013 by The American Society for Biochemistry and Molecular Biology, Inc.

Keywords

Amino Acid Motifs; Bacterial Toxins; Cholesterol; Exotoxins; Humans; Jurkat Cells; Lymphocyte Function-Associated Antigen-1; Membrane Microdomains; Pasteurellaceae; Protein Binding; Surface Plasmon Resonance

Disciplines

Dentistry

Author(s)

Angela C. Brown, Angela C. Balashova, Richard M. Epand, Raquel F. Epand, Alvina Bragin, Scott C. Kachlany, Michael J. Walters, Yurong Du, Kathleen Boesze-Battaglia, and Edward T. Lally

THE JOURNAL OF BIOLOGICAL CHEMISTRY VOL. 288, NO. 32, pp. 23607–23621, August 9, 2013

Aggregatibacter actinomycetemcomitans Leukotoxin Utilizes a Cholesterol Recognition/Amino Acid Consensus Site for Membrane Association*

Received for publication, May 17, 2013, and in revised form, June 20, 2013 Published, JBC Papers in Press, June 21, 2013, DOI 10.1074/jbc.M113.486654

Angela C. Brown[‡], Nataliya V. Balashova[§], Richard M. Epand[¶], Raquel F. Epand[¶], Alvina Bragin[‖], Scott C. Kachlany[§], Michael J. Walters[‡], Yurong Du[‡], Kathleen Boesze-Battaglia[‖], and Edward T. Lally[‡1]

From the Departments of [‡]Pathology and [‖]Biochemistry, University of Pennsylvania School of Dental Medicine, Philadelphia, Pennsylvania 19104, the [§]Department of Oral Biology, University of Medicine and Dentistry of New Jersey, Newark, New Jersey 07103, and the [¶]Department of Biochemistry and Biomedical Sciences, McMaster University, Hamilton, Ontario L8S 4K1, Canada

Background: A repeats-in-toxin (RTX) leukotoxin and its integrin receptor aggregate in cholesterol-rich lipid rafts.
Results: The affinity of the toxin to cholesterol is driven by a cholesterol recognition/amino acid consensus (CRAC) motif.
Conclusion: Leukotoxin cytotoxicity is regulated by the CRAC motif.
Significance: Other RTX toxins contain this CRAC motif, suggesting a role for cholesterol recognition in RTX cytolysis.

Aggregatibacter actinomycetemcomitans **produces a repeats-in-toxin (RTX) leukotoxin (LtxA) that selectively kills human immune cells. Binding of LtxA to its β_2 integrin receptor (lymphocyte function-associated antigen-1 (LFA-1)) results in the clustering of the toxin·receptor complex in lipid rafts. Clustering occurs only in the presence of LFA-1 and cholesterol, and LtxA is unable to kill cells lacking either LFA-1 or cholesterol. Here, the interaction of LtxA with cholesterol was measured using surface plasmon resonance and differential scanning calorimetry. The binding of LtxA to phospholipid bilayers increased by 4 orders of magnitude in the presence of 40% cholesterol relative to the absence of cholesterol. The affinity was specific to cholesterol and required an intact secondary structure. LtxA contains two cholesterol recognition/amino acid consensus (CRAC) sites; CRAC^{336} (^{333}LEEYSKR^{339}) is highly conserved among RTX toxins, whereas CRAC^{503} (^{501}VDYLK^{505}) is unique to LtxA. A peptide corresponding to CRAC^{336} inhibited the ability of LtxA to kill Jurkat (Jn.9) cells. Although peptides corresponding to both CRAC^{336} and CRAC^{503} bind cholesterol, only CRAC^{336} competitively inhibited LtxA binding to this sterol. A panel of full-length LtxA CRAC mutants demonstrated that an intact CRAC^{336} site was essential for LtxA cytotoxicity. The conservation of CRAC^{336} among RTX toxins suggests that this mechanism may be conserved among RTX toxins.**

Aggregatibacter actinomycetemcomitans is a pioneer colonizer of the upper aerodigestive tract of man. In the establishment of the ecological niche of the organism, it relies upon an array of virulence determinants, one of which is a leukotoxin (LtxA) that selectively kills human immune cells (1) in a process that is initiated by recognition of a cell surface molecule that leads to a multistep cascade and results in targeted cell death (2). LtxA is a member of the repeats-in-toxin (RTX)[2] family of cytotoxic proteins (3), which share cell type specificity that is driven by their association with β_2 integrin heterodimers, such as lymphocyte-function associated antigen-1 (LFA-1) (4) and macrophage-1 antigen (Mac-1)/complement receptor 3 (CR3) (5).

Five genes are required for successful translation and secretion of LtxA (the structural toxin gene product) in *A. actinomycetemcomitans*. Four of the genes, *ltx*CABD (in transcriptional order) are located in the leukotoxin operon. A fifth gene, *tde*A (6), is not part of the *ltx* operon and is located 572 kb downstream of this site. Prior to secretion, Gram-negative bacterial protein toxins are translated as protoxins and must be post-translationally modified to achieve biological activity. This modification takes various forms with bacterial protein toxins. In the case of RTX toxins, the RTXC protein, an acylase, catalyzes the attachment of fatty acyl chains to internal lysine residues of the toxin (7–9) in the bacterial cytoplasm; this acylation process is necessary for the toxin to achieve its biological activity (10). The remaining three gene products (LtxB, LtxD, and TdeA) form a type I secretion system and export LtxA directly from the bacterial cytoplasm to the external environment without the need for a periplasmic intermediate.

Hydropathy analysis of the amino acid sequence of LtxA (114.5 kDa; 1055 amino acids) (35, 36) in combination with algorithms predicting secondary structure (37, 38) permit the division of LtxA into four domains: hydrophobic, central, repeat, and C-terminal domains (35, 36) (Fig. 1*A*). The hydrophobic domain (residues 1–420) contains a preponderance of

* This work was supported, in whole or in part, by National Institutes of Health Grants R01DE009517 (to E. T. L.), F32DE020950 and K99DE022795 (to A. C. B.), and R01EY018705 and R01EY10420 (to K. B.-B.). This work was also supported by Canadian Institutes of Health Research Grant MOP 86608 (to R. M. E.).

[1] To whom correspondence should be addressed: Dept. of Pathology, University of Pennsylvania, School of Dental Medicine, 240 S. 40th St., 317 Levy Bldg., Philadelphia, PA 19104. Tel.: 215-898-5913; Fax: 215-898-2050; E-mail: lally@toxin.dental.upenn.edu.

[2] The abbreviations used are: RTX, repeats-in-toxin; LFA-1, lymphocyte function-associated antigen-1; CRAC, cholesterol recognition/amino acid consensus; SPR, surface plasmon resonance; DSC, differential scanning calorimetry; DMPC, 1,2-dimyristoyl-*sn*-glycero-3-phosphocholine; SOPC, 1-stearoyl-2-oleoyl-*sn*-glycero-3-phosphocholine; DOPC, 1,2-dioleoyl-*sn*-glycero-3-phosphocholine; GuHCl, guanidine hydrochloride.

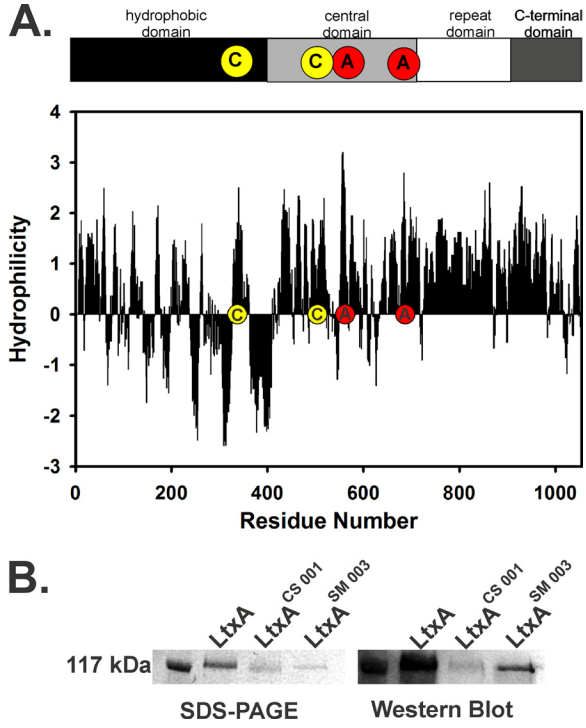

FIGURE 1. **Structure and purity of LtxA.** *A*, the sequence of LtxA contains an N-terminal hydrophobic domain, a central domain that contains two internal lysines (*red circle* labeled *A*) that are the sites of acylation, a repeat domain, and a C-terminal domain. The CRAC sites identified in this work are located near the hydrophobic region (*yellow circle* labeled *C*). *B*, SDS-PAGE gel and Western blot of $LtxA^{wt}$, $LtxA^{CS001}$, and $LtxA^{SM003}$.

hydrophobic amino acids and suggests an involvement in membrane insertion. Secondary structure predictions of the region show that half of the residues form either amphipathic or hydrophobic α-helices, which are often associated with toxin-target cell membrane interactions. Comparison of the amino acid sequence of LtxA with other RTX toxins, such as *Escherichia coli* α-hemolysin (HlyA) and *Mannheimia hemolytica* LktA, show a remarkable concordance in the clustering of hydrophobic and hydrophilic residues among the three toxins in this area (35, 36). The central domain (residues 421–730) is composed largely of hydrophilic residues, and the conservation of structure among the various RTX toxins is less strong. Located within the central region are the two acylated lysine residues (Lys^{562} and Lys^{687}) that are necessary for biological activity (10) (Fig. 1*A*, *red circles* labeled *A*). The repeat region (residues 730–900) contains a series of 14 repeated nonapeptides with the consensus sequence of GG*X*G(N/D)D*X*(L/I/F)*X* (where *X* represents any amino acid), which together form a unique calcium-binding structure that is called a parallel β-helix or parallel β-roll (39, 40). LtxA has been shown to bind calcium as well (41). Finally the C-terminal domain (positions 901–1055) is required for secretion (42).

The RTX toxins are known to be secreted into the aqueous solution but also to be membrane-interacting proteins (11). Neither the water-soluble nor the membrane-embedded structures of these toxins (and LtxA in particular) have been solved; however, it has been proposed that this family of toxins undergoes a conformational change upon membrane association (12). We have recently shown that LtxA undergoes distinct lipid-specific secondary structure changes upon binding to or disruption of lipid bilayers (13).

TABLE 1
Cytotoxicity of LtxA and Acylation Mutants

$LtxA^{wt}$, $LtxA^{renatured}$, $LtxA^{CS001}$ (nonacylated), and $LtxA^{SM003}$ (acylated) were incubated with Jn.9 cells. Cytotoxicity was measured using a trypan blue assay and was calculated as the number of cells killed relative to an untreated control. Each value represents the mean of three experiments ± standard deviation.

Protein	Cytotoxicity
	% untreated control
$LtxA^{wt}$	0.77 ± 0.08
$LtxA^{renatured}$	0.20 ± 0.15
$LtxA^{CS001}$	0.31 ± 0.24
$LtxA^{SM003}$	0.54 ± 0.08

LtxA and other RTX toxins bind to various β2 integrins and cluster in lipid rafts (14–16). The result of this interaction mimics aspects of the integrin (17) activation signal, including the elevation of cytosolic Ca^{2+}, activation of calpain, and cleavage of talin. The cleavage of talin frees LFA-1 from the cytoskeleton and allows lateral movement of the LFA-1·LtxA complex to lipid rafts (14). Although talin cleavage and release of LFA-1 is the initial step in toxin/integrin-driven raft clustering, the process that moves the LtxA·LFA-1 complex to the raft and subsequently maintains them in the raft is not clear. This observation has led us to hypothesize that LtxA has an affinity for cholesterol, a primary raft component, and this interaction may be responsible for the LtxA·LFA-1 clustering observed in intoxicated cells.

EXPERIMENTAL PROCEDURES

Chemicals—NaCl, $CaCl_2$, NaN_3, HEPES, cholesterol, guanidine hydrochloride (GuHCl), and KH_2PO_4 were purchased from Sigma. Lipids, including 1,2-dimyristoyl-*sn*-glycero-3-phosphocholine (DMPC), 1-stearoyl-2-oleoyl-*sn*-glycero-3-phosphocholine (SOPC), and 1,2-dioleoyl-*sn*-glycero-3-phosphocholine (DOPC), were purchased from Avanti Polar Lipids (Alabaster, AL). Ergosterol was purchased from MP Biomedicals (Solon, OH). Peptides were synthesized and purified (98% purity) by Biomatik (Wilmington, DE).

Bacterial Strains, Growth Conditions, and Plasmids—Three *A. actinomycetemcomitans* strains were used in this work, JP2, CS001, and SM003 (18). JP2 produces a wild type LtxA ($LtxA^{wt}$), CS001 lacks the *ltxC* gene and therefore produces an unacylated LtxA ($LtxA^{CS001}$), and SM003 has been complemented with the *ltxC* gene in trans and produces an acylated LtxA ($LtxA^{SM003}$). The *A. actinomycetemcomitans* strains were grown overnight in AAGM broth (19) supplemented with antibiotics (JP2: 12.5 μg/ml vancomycin and 75 μg/ml bacitracin, CS001: 40 μg/ml kanamycin, SM003: 40 μg/ml kanamycin and 2 μg/ml chloramphenicol). LtxA was purified as described previously (20). The purity of the toxin was confirmed by Coomassie staining of SDS-PAGE and the specificity by cross-reactivity with anti-LtxA antibody (Western blot). We confirmed the activity using a cytotoxicity assay. The purity of the three proteins is shown in Fig. 1*B*, and the cytotoxicity is shown in Table 1.

Production of CRAC mutant LtxA was accomplished in *E. coli* using a pSHH plasmid, a pUC19-based plasmid contain-

TABLE 2
Primers used for site-directed mutagenesis of ltxA
The substituted nucleotides are in bold type.

Primer	Sequence	Mutation site
ltxA_1012_FW	5′-AGAATGCTTGAGGAA**CC**CTCGAAACGCTTTAA-3′	CRAC336
ltxA_1012_RV	5′-TTAAAGCGTTTCGAG**GG**TTCCTCAAGCATTCT-3′	CRAC336
ltxA_1513_FW	5′-AAAGCTTATGTGGAT**CC**TTTGAAAAAGGGTGA-3′	CRAC503
ltxA_1513_RV	5′-TCACCCTTTTTCAAA**GG**ATCCACATAAGCTTT-3′	CRAC503

ing the *ltxA* promoter, *ltx*C, and *ltx*A (21). Active LtxA is constitutively expressed in the cytosol.

The CRAC mutants were constructed by substituting proline for tyrosine at amino acid positions 336 (for $CRAC^{Y336P}$) or 503 (for $CRAC^{Y503P}$) of *ltxA*. Site-directed mutagenesis was performed using a QuikChange® site-directed mutagenesis kit (Agilent Technologies, Inc., Santa Clara, CA), according to the manufacturer's instructions. The primers containing substitutions were designed using the OligoPerfect™ Designer as shown in Table 2. The reactions were performed on an automated thermal cycler with an initial step of 30 s at 95 °C, followed by PCR amplification for 16 cycles of 30 s at 95 °C, 1 min at 55 °C, and 3 min at 68 °C. The obtained PCR products were transformed into DH5α-T1 cells, and the mutant clones were selected on LB agar plates with 50 μg/ml of ampicillin.

$CRAC^{Y336P}$ and $CRAC^{Y503P}$ were produced from *E. coli* using the following procedure. Overnight cultures of *E. coli* DH5α-T1 containing the plasmid were used at a 1:50 dilution to inoculate 200 ml of LB/ampicillin (50 μg/ml), which was grown to an A_{600} of ~0.4. The cultures were centrifuged and resuspended in 6 ml of buffer (20 mM Tris-HCl, 250 mM NaCl, 0.2 mM $CaCl_2$, pH 6.8), sonicated (six times for 45 s, on ice), and centrifuged to remove cell debris (12,000 × *g*, 15 min, 4 °C).

LtxA ($LtxA^{renatured}$) was denatured by incubating 1 μM $LtxA^{wt}$ with an equal volume of 16 M GuHCl overnight (12). Following incubation, the GuHCl was exchanged with liposome buffer (150 mM NaCl, 5 mM $CaCl_2$, 5 mM HEPES, and 3 mM NaN_3, pH 7.4) for use in the SPR experiments.

Cell Culture—Jn.9, a subclone of the Jurkat cell line (22), a gift from Dr. Lloyd Klickstein (Novartis Institute for Biomedical Research, Cambridge, MA), was maintained as described previously (14) with 2 mM L-glutamine and 50 μg/ml gentamicin.

Liposome Preparation—Lipids dissolved in chloroform were added to a glass vial in the required amounts (24). The chloroform was evaporated under a stream of nitrogen, and the residual chloroform was removed under vacuum, creating a thin lipid film on the glass surface. Liposomes were created by hydrating the lipid film with liposome buffer (150 mM NaCl, 5 mM $CaCl_2$, 5 mM HEPES, 3 mM NaN_3, pH 7.4). Large unilamellar vesicles were formed by extruding the liposome solutions through a 200-nm polycarbonate membrane (24, 25).

The lipid compositions used in this work were chosen based on their raft-like nature (26). The liposomes were composed of DMPC with 0, 20, 40, or 60% cholesterol (or ergosterol). At room temperature, DMPC with 0% cholesterol exists in a non-raft-like state (liquid disordered); at 40 and 60% cholesterol, DMPC exists in a raft-like state (liquid ordered); and at 20% cholesterol, both phases coexist (27, 28).

Circular Dichroism Spectroscopy—The extent of unfolding of $LtxA^{renatured}$ was determined using CD spectroscopy. Three LtxA samples were prepared at a concentration of 7 μM. 1) Native $LtxA^{wt}$ was suspended in liposome buffer, 2) $LtxA^{denatured}$ was prepared as described above (12) and left in GuHCl, and 3) $LtxA^{renatured}$ was prepared as described above, and the buffer was exchanged with liposome buffer (to recreate the conditions of the SPR experiment).

CD spectroscopy analysis was performed on a Jasco J-810 spectropolarimeter, as discussed in our previous studies (13). The samples were analyzed at 25 °C in a 0.2-mm-path length quartz cell using the step-scanning mode from 260 to 200 nm, with a 1-nm wavelength step, 10-s averaging time, and 1-nm bandwidth. The spectra were recorded under identical conditions for an $n = 3$ for each sample.

Surface Plasmon Resonance—Liposomes were tethered to an L1 Biacore chip by flowing them over the chip at a rate of 5 μl/min, until a mass corresponding to ~1000 response units (~5 μl) had been added to the surface (30). A small volume of NaOH (5 μl) was added to remove unbound liposomes.

For kinetic analysis, the flow rate was increased to 30 μl/min before the toxin injection was initiated. Each toxin injection was 60 μl, followed by a 180-μl dissociation of buffer only. The surface was regenerated with an injection of 65 μl of 0.5% SDS. The 10 toxin concentrations ranged from 0 to 500 nM in a 1:2 dilution series. All SPR measurements were performed on a Biacore® 3000, and the data were evaluated using the BIAevaluation® software. The data were fit using a 1:1 Langmuir binding model to obtain the equilibrium dissociation constant (K_D), as well as the association (k_a) and dissociation (k_d) rates, where K_D is given by the following equation.

$$K_D = \frac{k_d}{k_a} \qquad \text{(Eq. 1)}$$

For steady state competition analysis, liposomes containing 40% cholesterol were tethered to an L1 chip. The flow rate was set at 5 μl/min, and 50 μl of toxin was injected, followed by a 25-μl dissociation of buffer only. The surface was regenerated with SDS, as described above. In the CRAC peptide competition experiments, the toxin, at a concentration of 1000 nM, was incubated with an equal volume of peptide at concentrations of 0, 500, 1000, 2000, and 4000 nM (molar LtxA:peptide ratios of 1:0, 1:0.5, 1:1, 1:2, and 1:4). The inhibition was defined as follows,

$$\%\text{Inhibition} = \frac{RU_{LtxA/peptide}}{RU_{LtxA}} \times 100 \qquad \text{(Eq. 2)}$$

where R_{LtxA} is the response units of the LtxA-only run, and $RU_{LtxA/peptide}$ is the response units of each run containing LtxA and peptide. Response units represent the surface coverage. The response units were measured at the end of the injection,

just before the dissociation was initiated, at the same time point for each experiment. In the comparison of binding to cholesterol-containing liposomes by the acylation mutant toxins, $LtxA^{CS001}$ and $LtxA^{SM003}$, at concentrations of 250 nM, were injected over liposomes containing 40% cholesterol that had been tethered to the L1 chip.

Differential Scanning Calorimetry—The DSC experiments were performed as described previously (31), with the following modifications. Approximately 1 mg of the dried peptide was resuspended in 100 μl of methanol and added to a solution of SOPC with or without cholesterol in chloroform:methanol (2:1) to give the desired final ratio of peptide to lipids. The solvent was removed under nitrogen gas, and the final traces of solvent were removed in a vacuum desiccator. The films were hydrated with PIPES buffer (20 mM PIPES, 140 mM NaCl, 1 mM EDTA, adjusted to pH 7.4) and vortexed extensively. The suspension was degassed and loaded into the sample cell of a Nano II differential scanning calorimeter (Calorimeter Sciences Corp., Lindon, UT). Buffer was placed in the reference cell. Successive heating and cooling scans were run between 0 and 45 °C, at a scan rate of 1°/min.

Cytotoxicity—A trypan blue cytotoxicity assay was used to measure cell viability (32). The percentage of cells killed by each treatment was calculated by the following,

$$\%\text{kill} = \frac{\#_{t=0} - \#_{t=5}}{\#_{t=0}} \qquad \text{(Eq. 3)}$$

where $\#_{t=0}$ is the number of cells before treatment, and $\#_{t=5}$ is the number of cells after treatment. Each %kill value was normalized to the %kill value of LtxA alone.

The effect of the CRAC peptides on LtxA-mediated cell death was measured in cytotoxicity assays, as described previously (14). Briefly, Jn.9 cells were incubated with protein samples containing (*a*) LtxA (1×10^{-8} M), (*b*) LtxA (1×10^{-8} M) + peptide (1×10^{-8} M), or (*c*) peptide (1×10^{-8} M). The samples were incubated at 37 °C for 5–24 h.

In the case of the full-length LtxA CRAC mutants, 50 μg of total protein in the *E. coli* cytosolic fraction was added to 0.5×10^6 Jn.9 cells and incubated for 24 h. Cell death was measured with a trypan blue assay using a Vi-cell machine (Beckman Coulter, Hialeah, FL). Western blot analysis was used to confirm LtxA expression. An *E. coli* DH5α-T1 cytosolic fraction that did not contain pSHH served as a control.

Statistical Analysis—The statistical analyses were performed using either Student's *t* test or one-way analysis of variance using SigmaPlot® (Systat Software, Inc. Chicago, IL). The following statistical criteria were applied: $p < 0.001$, $p < 0.05$, and $p < 0.01$.

RESULTS

LtxA Has a Strong Affinity for Cholesterol—Fig. 2 shows the affinity of LtxA for liposomes containing DMPC and varying amounts of cholesterol (reported as mol %). Using SPR, we measured the binding of LtxA to membranes containing 0, 20, 40, or 60% cholesterol as a function of time (Fig. 2, *A*, *B*, *C*, and *D*, respectively).

These SPR sensorgrams were used to calculate the kinetic parameters of binding. The affinity of LtxA for the membranes increased (K_D decreased) as the amount of cholesterol increased up to 40% and then decreased (K_D increased) in membranes containing 60% cholesterol (Fig. 2*E*). The maximal affinity (minimal K_D) to membranes containing 40% cholesterol was approximately 4 orders of magnitude greater (10^{-12} M) than the affinity for cholesterol-free membranes (10^{-8} M).

Table 3 shows the corresponding association (k_a) and dissociation (k_d) rates for the binding of LtxA to liposomes containing 0–60% cholesterol. There was no significant change in the association rate as the amount of cholesterol increased; however, the dissociation rate decreased as the amount of cholesterol in the membranes increased to 40% and then increased at 60% cholesterol. Therefore, the affinity of LtxA to cholesterol, as measured by the K_D, is almost entirely due to cholesterol-dependent changes in the dissociation rate rather than changes in the association rate.

Binding Is Specific for Cholesterol—We then compared the affinity of LtxA for liposomes composed of DMPC and varying amounts of the sterol ergosterol (substituted for cholesterol) as a specificity control. The structures of these two sterols are similar, with ergosterol containing an additional double bond in the B ring and a double bond on carbon 22. The SPR sensorgrams showing LtxA association to and dissociation from membranes containing 0, 20, 40, and 60% ergosterol are shown in Fig. 2 (*F*, *G*, *H*, and *I*, respectively).

As shown in Fig. 2*J*, the K_D values remained essentially constant as the ergosterol composition increased, with no strong affinity observed at high sterol compositions. In Fig. 2, the difference between *panels E* and *J* indicates that the strong affinity of LtxA to sterol-containing membranes is specific for cholesterol. Membranes composed of DMPC and cholesterol are known to phase separate into cholesterol-poor (liquid-disordered) and cholesterol-rich (liquid-ordered) regions, depending on the temperature and cholesterol composition of the system (28). The liquid-ordered phase is often used as a model of lipid rafts because of their similar compositions (rich in cholesterol and saturated lipids, poor in unsaturated lipids).

To determine whether the affinity of LtxA for cholesterol-containing membranes is determined by the cholesterol composition or by the raft-like nature of the membrane, we compared the affinity of LtxA for membranes composed of 60% DOPC (unsaturated)/40% cholesterol, a lipid composition that is liquid-disordered (non-raft-like), with membranes composed of 60% DMPC (saturated)/40% cholesterol, a lipid composition that is liquid-ordered (raft-like). The SPR sensorgrams showing LtxA association to and dissociation from membranes containing DMPC/40% cholesterol or DOPC/40% cholesterol are shown in Fig. 2 (*K* and *L*, respectively). The affinity of LtxA for membranes containing 40% cholesterol was not significantly different for the two lipid types (Fig. 2*M*), demonstrating that it is the presence of cholesterol that regulates this strong affinity rather than the raft-like nature of the membrane.

To determine whether a specific LtxA structural element regulates the affinity of the toxin for cholesterol, we studied the binding of renatured LtxA ($LtxA^{renatured}$) to DMPC membranes containing varying amounts of cholesterol. The binding of $LtxA^{renatured}$ to membranes containing 0, 20, 40, or 60% cholesterol as a function of time is shown in Fig. 3 (*A*, *B*, *C*, and *D*,

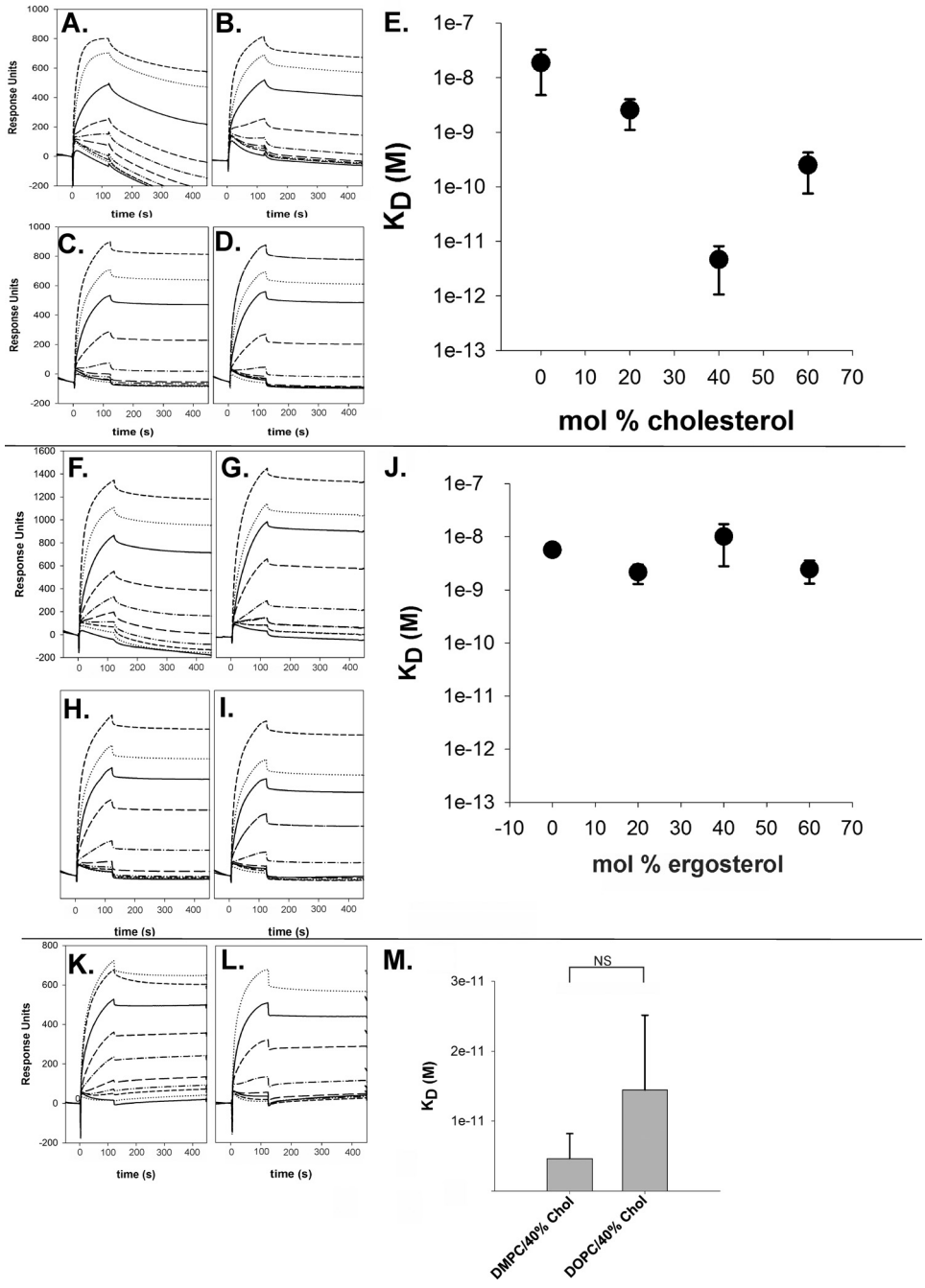

FIGURE 2. **Affinity of LtxA^{wt} for sterol-containing membranes.** Liposomes containing 0, 20, 40, or 60% sterol were tethered to an L1 Biacore chip, and LtxA^{wt} was injected over the top. *A–D*, The sensorgrams show LtxA^{wt} binding to membranes containing 0% cholesterol (*A*), 20% cholesterol (*B*), 40% cholesterol (*C*), and 60% cholesterol (*D*). *E*, the binding affinity (K_D) of LtxA^{wt} for cholesterol was calculated from these sensorgrams. A one-way analysis of variance test demonstrated that the data in *E* are significant ($p < 0.05$). *F–I*, a second series of sensorgrams shows the binding of LtxA to membranes containing 0% ergosterol (*F*), 20% ergosterol (*G*), 40% ergosterol (*H*), and 60% ergosterol (*I*). *J*, the binding affinity (K_D) of LtxA for ergosterol was calculated from these sensorgrams. A one-way analysis of variance test indicates that there is no significant difference in the data ($p = 0.097$). *K* and *L*, the third set of sensorgrams shows the binding of LtxA^{wt} to membranes containing DMPC/40% cholesterol (*K*) and DOPC/40% cholesterol (*L*). *M*, the affinity of LtxA^{wt} for liposomes containing 40% cholesterol and either the saturated lipid, DMPC, or the unsaturated lipid, DOPC, is not significantly different ($p = 0.207$). These two lipid systems contain the same amount of cholesterol but differ in their raft-like nature, with DMPC/40% cholesterol existing in a raft-like state and DOPC/40% cholesterol existing in a non-raft-like state. The data in *E*, *J*, and *M* represent the averages of three independent experiments, and the *error bars* represent the standard deviation. The data in *A–D*, *F–I*, and *K–L* are representative plots.

respectively). As shown in Fig. 3*E*, similarly to folded LtxA, the affinity of LtxA^{renatured} reached a maximum at 40% cholesterol (minimum in K_D); however, this maximum is less pronounced (by 3 orders of magnitude) than the maximum affinity of native LtxA for cholesterol-containing membranes (Fig. 2*E*) and is not statistically significant. Table 3 shows the corresponding association (k_a) and dissociation (k_d) rates.

The extent of LtxA unfolding with GuHCl in the LtxA^{renatured} sample was analyzed by CD. As shown in the *inset* of Fig. 3*E*, the CD spectra of LtxA^{wt} (*solid lines*) indicated that the protein was

folded and contained some secondary structure. In contrast, the CD spectra of LtxA^{denatured} in 8 M GuHCl (*dashed lines*) shows that the GuHCl has unfolded the protein. After GuHCl exchange with liposome buffer, LtxA^{renatured} (*dotted lines*) adopted a similar, but distinct shape as LtxA^{wt}, indicating that the toxin remains partially unfolded. The final GuHCl concentration in the liposome buffer-exchanged sample was 2 M; previous work has shown that at this GuHCl concentration, LtxA loses its ability to kill target cells (12). However, these results suggest that the secondary structure of LtxA is not essential for its binding to cholesterol.

LtxA Affinity for Cholesterol Is Independent of Its Acylation Status—LtxA is post-translationally modified by the addition of two fatty acid chains to two internal lysines (10). For some proteins, acylation has been proposed to enhance membrane association (34). We therefore investigated whether the association of LtxA with cholesterol depends on the presence of the acyl groups by using a nonacylated mutant (LtxA^{CS001}) and a reconstructed mutant (LtxA^{SM003}). The purity and cytotoxicity of these mutants is shown in Fig. 1*B* and Table 1. We measured the binding of these mutant toxins to cholesterol using a steady state SPR assay. The SPR sensorgrams are shown in Fig. 4*A*, and the maximal response units (a measure of binding) are shown in Fig. 4*B*. Binding to cholesterol was enhanced in the absence of acyl chains, relative to the fully acylated protein, LtxA^{SM003}, indicating that acylation is not responsible for the strong affinity of LtxA for cholesterol, and it may actually inhibit binding to cholesterol.

TABLE 3

Kinetic parameters of LtxA^{wt} and LtxA^{renatured} binding to liposomes containing varying cholesterol compositions

LtxA^{wt} or LtxA^{renatured} was injected over liposomes composed of varying amounts of cholesterol tethered to a L1 chip. The rates of association and dissociation (k_a and k_d, respectively) were fit to a 1:1 Langmuir binding model, using the BIAevaluation software. The values represent the means of four independent experiments ± standard deviation.

	k_a	k_d
LtxA^{wt}	$M^{-1}s^{-1}$	s^{-1}
0% cholesterol	$7.68 \pm 4.38 \times 10^4$	$7.51 \pm 3.95 \times 10^{-4}$
20% cholesterol	$7.32 \pm 1.63 \times 10^4$	$3.10 \pm 2.26 \times 10^{-4}$
40% cholesterol	$6.05 \pm 0.88 \times 10^4$	$3.00 \pm 2.59 \times 10^{-7}$
60% cholesterol	$6.31 \pm 1.43 \times 10^4$	$3.10 \pm 3.09 \times 10^{-5}$
LtxA^{renatured}		
0% cholesterol	$7.39 \pm 3.27 \times 10^4$	$1.54 \pm 1.01 \times 10^{-3}$
20% cholesterol	$6.68 \pm 2.24 \times 10^4$	$1.53 \pm 0.03 \times 10^{-4}$
40% cholesterol	$6.33 \pm 3.10 \times 10^4$	$5.48 \pm 2.47 \times 10^{-5}$
60% cholesterol	$3.76 \pm 1.82 \times 10^4$	$9.37 \pm 3.83 \times 10^{-5}$

LtxA Contains CRAC Sites—The high affinity binding of LtxA to cholesterol suggests the presence of a lipid binding site(s) within the LtxA protein. We scanned the LtxA amino acid sequence of the toxin for the (L/V)X_{1-5}YX_{1-5}(R/K) CRAC site motif (43), which has been shown to be associated with cholesterol binding. We identified two putative CRAC sites within the LtxA sequence: CRAC^{336} (^{333}LEEYSKR^{339}) and CRAC^{503} (^{501}VDYLK^{505}) (Fig. 1*A*, *yellow circles* labeled *C*). CRAC^{336} is located within the hydrophobic region and is highly conserved among several RTX toxins, including *E. coli* HlyA, *M. hemolytica* leukotoxin, *Actinobacillus pleuropneumoniae* AppA, and *A. pleuropneumoniae* hemolysin (Table 4). CRAC^{503} is not conserved with other RTX toxins, although *E. coli* HlyA has some homology in that region. *Bordetella pertussis* adenylate cyclase toxin (CyaA) does not share either CRAC motif with other RTX toxins, although the deduced amino acid sequence does contain five putative CRAC sites.

CRAC Peptides Inhibit Cholesterol Binding by LtxA—Synthetic peptides corresponding to the CRAC^{336} and CRAC^{503} sequences were synthesized (Table 5). The first set of peptides (CRAC^{336}) corresponds to the CRAC site between residues 333 and 339, and the second set (CRAC^{503}) corresponds to the CRAC site between residues 501 and 505. Within each set, peptide "WT" is the wild type sequence, peptide "MUT" contains a proline in place of the central tyrosine residue (the central tyrosine has been shown to be critical for cholesterol binding (44)), and peptide "SCM" contains the scrambled CRAC sequence.

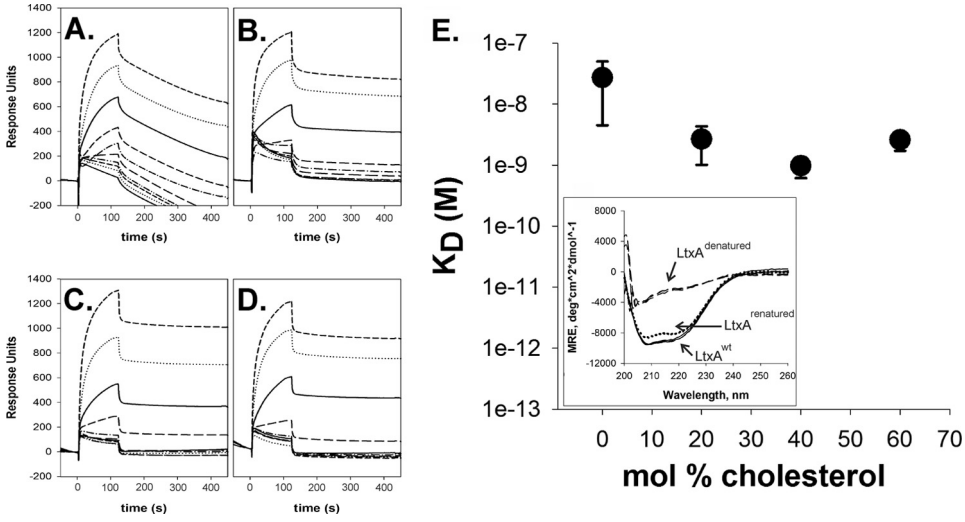

FIGURE 3. **Affinity of LtxA^{renatured} for cholesterol.** Liposomes containing 0, 20, 40, or 60% cholesterol were tethered to an L1 Biacore chip, and LtxA^{renatured} was injected over the top. *A–D*, The sensorgrams show LtxA^{renatured} binding to membranes containing 0% cholesterol (*A*), 20% cholesterol (*B*), 40% cholesterol (*C*), and 60% cholesterol (*D*). *E*, the binding affinity (K_D) of LtxA^{renatured} was calculated from these sensorgrams. The CD spectra of LtxA^{wt} (*solid line*), LtxA^{denatured} in 8 M GuHCl (*dashed lines*), and LtxA^{renatured} (*dotted lines*) in liposome buffer are shown in the *inset* of *E*. A one-way analysis of variance test indicates that there is no significant difference in the data ($p = 0.063$). The data in *E* represent the averages of four independent experiments, and the *error bars* represent the standard deviation. The data in *A–D* are representative plots.

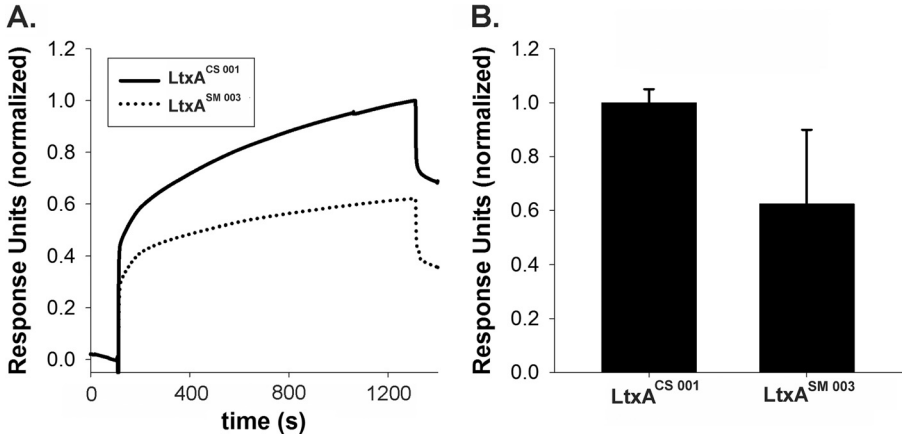

FIGURE 4. **Effect of LtxA acylation on binding to cholesterol.** Liposomes containing 40% cholesterol were tethered to an L1 Biacore chip, and acylated or nonacylated LtxA was injected over the top. *A*, steady state SPR binding by nonacylated toxin (LtxA^{CS001}, *solid line*) and acylated toxin (LtxA^{SM003}, *dashed line*) to liposomes containing 40% cholesterol. *B*, normalized response units (indicating extent of binding) at $t = 2100$ s for both protein types. The difference between the two data points is not significant. The data in *A* and *B* represent the averages of three independent experiments, and the *error bars* represent the standard deviation.

TABLE 4

RTX CRAC site homology

Sequence homology of the two CRAC sites in LtxA with other RTX toxins. Each CRAC site is bold and underlined.

Toxin	Sequence
CRAC^{336}	
A. actinomycetemcomitans (LtxA)[a]	^{332}M**LEEYSKR**FK^{341}
E. coli (HlyA)[b]	^{320}Q**LESYSER**FK^{329}
M. haemolytica (LktA)[c]	^{334}S**LESYAER**FK^{343}
A. pleuropneumoniae (AppA)[d]	^{330}L**IKSYSER**FQ^{339}
A. pleuropneumoniae (HlyA)[e]	^{330}Q**LEQYSER**FK^{339}
B. pertussis (CyaA)[f]	^{634}QLDKLAQESS^{643}
CRAC^{503}	
A. actinomycetemcomitans (LtxA)[a]	^{499}AY**VDYLK**KGE^{508}
E. coli (HlyA)[b]	^{487}AY**INYLE**NGG^{496}
M. haemolytica (LktA)[c]	^{493}AYVDAFEEGQ^{502}
A. pleuropneumoniae (AppA)[d]	^{497}AYVDAFEEGQ^{506}
A. pleuropneumoniae (HlyA)[e]	^{497}AYVDFFEEGK^{506}
B. pertussis (CyaA)[f]	^{801}VFVDRFVQGE^{810}

[a] Sequence accession number CAA34731.
[b] Sequence accession number AAC24352.
[c] Sequence accession number Q9EV31.
[d] Sequence accession number 123196.
[e] Sequence accession number 1710793.
[f] Sequence accession number 34978355.

TABLE 5

LtxA CRAC peptides

A panel of two sets of peptides was created to correspond to LtxA CRAC^{336} and CRAC^{503} sequences. Each set contained peptides corresponding to the wild type CRAC sequence (WT), the CRAC sequence with the Tyr replaced by Pro (MUT), and the scrambled CRAC sequence (SCM).

Peptide	Mutation	Sequence
CRAC^{336WT}	None	NH_2-FDRARM**LEEYSKR**FKKFGY-*OH*
CRAC^{336MUT}	Tyr → Pro	NH_2-FDRARM**LEEPSKR**FKKFGY-OH
CRAC^{336SCM}	Scrambled	NH_2-FDRARM**YEKLERS**FKKFGY-OH
CRAC^{503WT}	None	NH_2-QSGKAY**VDYLK**KGEELA-OH
CRAC^{503MUT}	Tyr → Pro	NH_2-QSGKAY**VDPLK**KGEELA-OH
CRAC^{503SCM}	Scrambled	NH_2-QSGKAY**YKLDV**KGEELA-OH

The interaction of each of these peptides with cholesterol-containing membranes was measured using DSC. The peptide-induced rearrangement of cholesterol in a membrane into cholesterol-rich domains can be followed by measuring the formation of cholesterol crystallites when the sterol passes its solubility limit. The formation of these crystallites can be readily detected with DSC through their polymorphic thermal transition, which occurs with a characteristic hysteresis, appearing at ~35 °C in heating scans and at ~23 °C in cooling scans at most conventional scan rates (45).

TABLE 6

Enthalpy of SOPC gel to liquid transition with 15 mol % peptide

Each of the six CRAC peptides was incubated with liposomes containing SOPC at 15 mol % peptide.

Peptide	Mutation	T_m	ΔH[a]
		°C	*kcal/mol*
None		3.7	4.00
CRAC^{336WT}	None	3.6	4.00
CRAC^{336MUT}	Tyr → Pro	3.6	4.18
CRAC^{336SCM}	Scrambled	3.6	4.25
CRAC^{503WT}	None	3.7	4.13
CRAC^{503MUT}	Tyr → Pro	3.7	3.40
CRAC^{503SCM}	Scrambled	3.7	3.49

[a] The transition temperature (T_m) and enthalpies (ΔH) were calculated as the average from the cooling scans only (because the heating scans did not reach a stable base line at low temperatures before the peak where heating was initiated).

As shown in Table 6, none of the CRAC peptides caused a change in the phase transition temperature of pure SOPC in the absence of cholesterol at a peptide mol fraction of 0.15. In addition, none of the CRAC^{336} peptides caused any substantial change in the gel to liquid crystalline phase transition enthalpy, nor did CRAC peptide^{503WT}. However, peptides CRAC^{503MUT} and CRAC^{503SCM} both lowered the transition enthalpy by ~20%. Thus, two of the non-CRAC negative control peptides, CRAC^{503MUT} and CRAC^{503SCM}, have some interaction with SOPC, corresponding to a more hydrophobic peptide. However, by the DSC criterion, all of the other peptides have little effect on the pure lipid, as shown in Fig. 5, and thus neither of the CRAC peptides, CRAC^{336WT} or CRAC^{503WT}, penetrate deeply into the bilayer in the absence of cholesterol.

With mixtures of SOPC and cholesterol at a molar ratio of 6:4, 15 mol % of each of the six peptides was used. No cholesterol crystallite transitions were observed in SOPC:cholesterol 6:4 in the absence of peptide, as observed by the absence of the characteristic transitions at 35 °C on heating and at 23 °C on cooling. In the presence of 15 mol % peptide, the characteristic transitions were observed for all peptides, as shown in Table 7 and Fig. 6. The greatest enthalpies of these cholesterol crystallite transitions were observed with the two CRAC peptides,

$CRAC^{336WT}$ and $CRAC^{503WT}$ (Table 7). These DSC results indicate that both CRAC peptides ($CRAC^{336WT}$ and $CRAC^{503WT}$) interact with cholesterol more strongly than do the control peptides ($CRAC^{336MUT}$, $CRAC^{336SCM}$, $CRAC^{503MUT}$, and $CRAC^{503SCM}$).

To determine whether the interaction of the CRAC peptides with cholesterol inhibits binding of LtxA to cholesterol, a series of SPR competition experiments was run. In each experiment, LtxA was incubated with increasing amounts of each CRAC peptide (molar LtxA:peptide ratios of 1:0, 1:0.5, 1:1, 1:2, and 1:4), and this mixture was injected over tethered liposomes containing 40% cholesterol.

TABLE 7

Enthalpy of cholesterol crystallite transitions

Each of the six CRAC peptides was incubated with liposomes containing SOPC and cholesterol (6:4) at 15 mol % peptide. The formation of cholesterol crystallites was observed by the characteristic hysteresis at approximately 35 °C in heating scans and at approximately 23 °C in cooling scans.

Peptide	Mutation	ΔH_{heat}	ΔH_{cool}	ΔH_{avg} [a]
		cal/mol	*cal/mol*	*cal/mol*
$CRAC^{336WT}$	None	160	140	150
$CRAC^{336MUT}$	Tyr → Pro	100	80	90
$CRAC^{336SCM}$	Scrambled	80	60	70
$CRAC^{503WT}$	None	190	170	180
$CRAC^{503MUT}$	Tyr → Pro	95	75	85
$CRAC^{503SCM}$	Scrambled	60	60	60

[a] The average transition enthalpies (ΔH_{avg}) were calculated as the averages from the heating and cooling scans.

Fig. 7*A* demonstrates that $CRAC^{336WT}$ inhibited binding of LtxA to cholesterol. The $CRAC^{336MUT}$ (Fig. 7*B*) control peptide only slightly inhibited binding of LtxA to cholesterol, and the $CRAC^{336SCM}$ (Fig. 7*C*) control peptide slightly enhanced binding of LtxA to cholesterol. As shown in Fig. 7*D*, $CRAC^{503WT}$ had a minimal effect on the binding of LtxA to cholesterol. The $CRAC^{503MUT}$ peptide had an even slighter inhibitory effect on binding, and $CRAC^{503SCM}$ slightly increased the binding of LtxA to cholesterol, as shown in Fig. 7 (*E* and *F*, respectively). The effects of all three $CRAC^{503}$ peptides were statistically insignificant ($CRAC^{503WT}$, $p > 0.096$; $CRAC^{503MUT}$, $p > 0.284$; $CRAC^{503SCM}$, $p > 0.390$). The hydrophobic nature of these six peptides may have some effect on the binding of LtxA to the membrane, but it is clear that the largest and most significant effect is the inhibition of binding to cholesterol by $CRAC^{336WT}$.

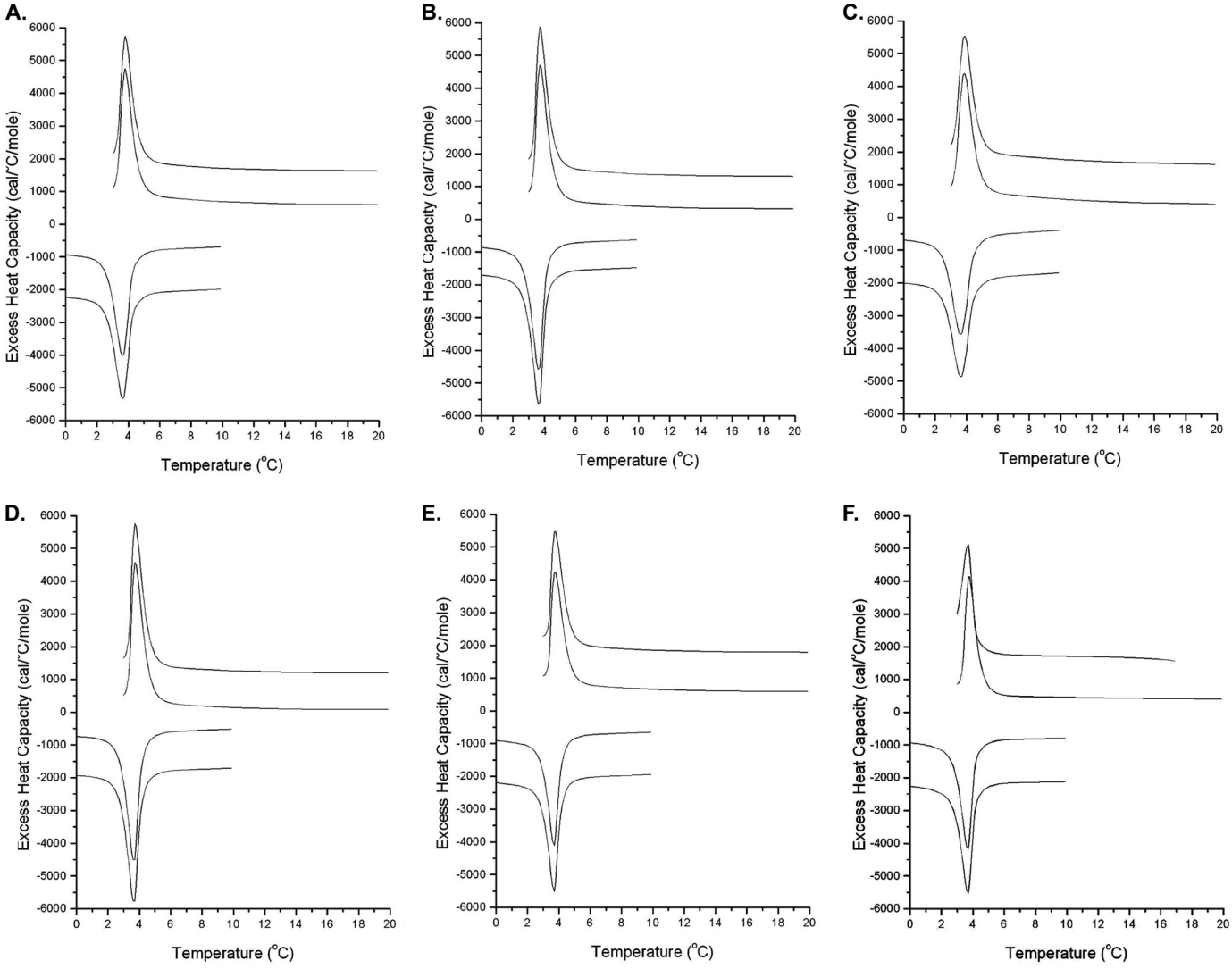

FIGURE 5. **DSC scans showing the gel-to-liquid crystalline transition temperatures.** Liposomes composed of 100% SOPC were mixed with 15 mol % CRAC peptides. *A*, $CRAC^{336WT}$; *B*, $CRAC^{336MUT}$; *C*, $CRAC^{336SCM}$; *D*, $CRAC^{503WT}$; *E*, $CRAC^{503MUT}$; *F*, $CRAC^{503SCM}$. *Positive curves* are heating scans, and *negative curves* are cooling scans. The *curves* were displaced along the *y* axis for ease of presentation. The scan rate was 1°/min.

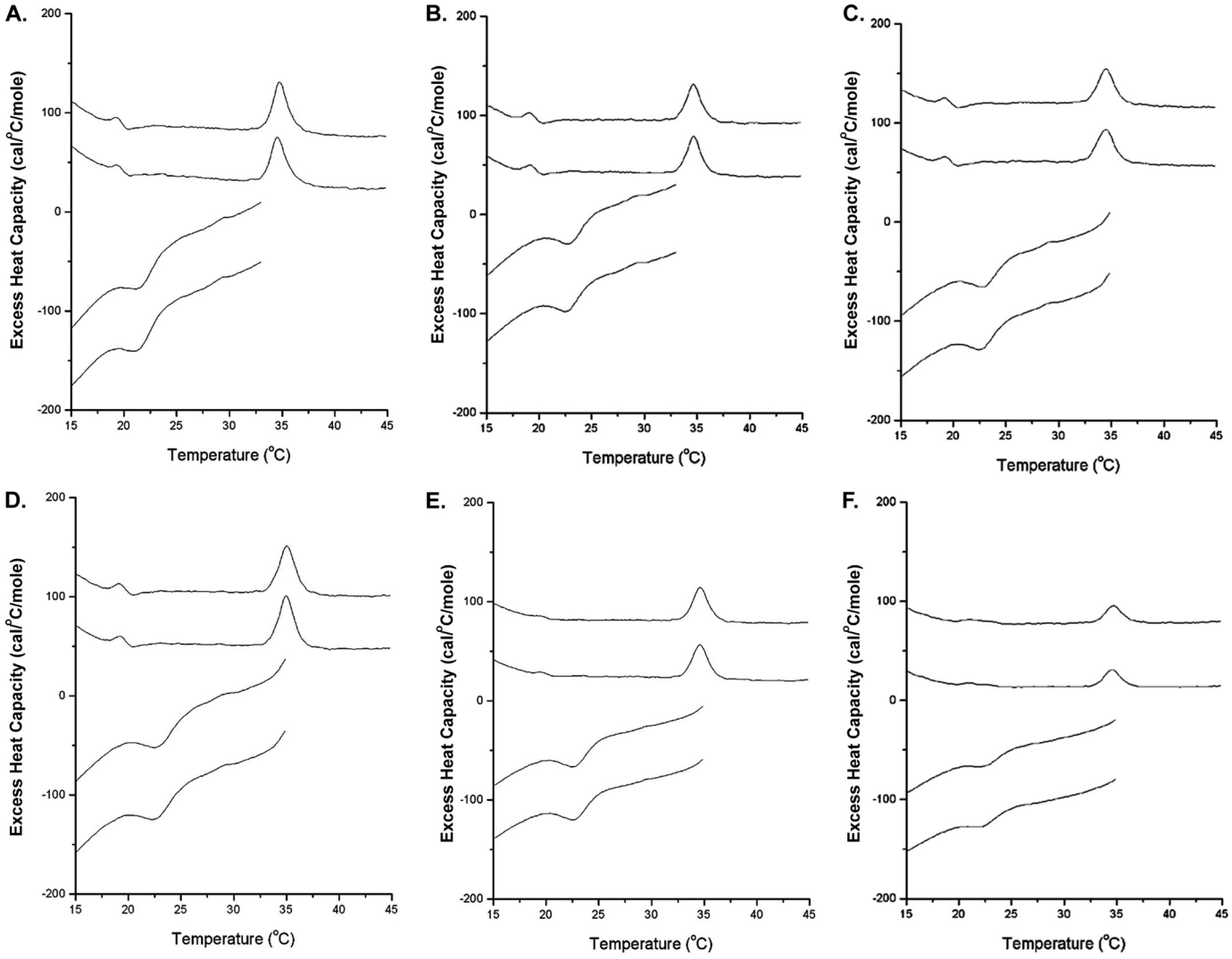

FIGURE 6. **DSC scans showing the characteristic cholesterol crystallite transitions at 35 °C on heating and 23 °C on cooling.** The lipid mixture was SOPC:cholesterol 6:4, containing 15 mol % CRAC peptide. *A*, CRAC^{336WT}; *B*, CRAC^{336MUT}; *C*, CRAC^{336SCM}; *D*, CRAC^{503WT}; *E*, CRAC^{503MUT}; *F*, CRAC^{503SCM}. *Positive curves* are heating scans, and *negative curves* are cooling scans. The *curves* were displaced along the *y* axis for ease of presentation. The scan rate was 1°/min.

Collectively, these results suggest that CRAC^{336} is involved in the binding of cholesterol by LtxA, but CRAC^{503} is not. The inhibition of binding by the CRAC^{336} and CRAC^{503} peptides is shown in Fig. 7 (*G* and *H*, respectively).

In addition, the specificity of the inhibition of CRAC^{336WT} on binding to cholesterol was demonstrated by injecting the LtxA/CRAC^{336WT} mixtures over liposomes containing no cholesterol (100% DMPC). Here (Fig. 7*I*), no inhibition of binding was observed, indicating that this peptide inhibits binding only when cholesterol is present in the membrane, and therefore, the peptide's binding to cholesterol is what drives the observed inhibition of LtxA binding.

LtxA Binding to Cholesterol Is Required for Cytotoxicity—The effect of the CRAC peptides on the LtxA-mediated cytotoxicity of Jn.9 cells was measured. Each set of cells was incubated for 5 h with either PBS, LtxA, LtxA:CRAC peptide (1:2), or CRAC peptide alone.

Table 8 shows the % cytotoxicity values, normalized to LtxA-induced cytotoxicity, which was set as 1.00. CRAC^{336WT}, which inhibits LtxA binding to cholesterol, almost completely eliminated LtxA-mediated cell death (% cytotoxicity = 0.06). CRAC^{336MUT} and CRAC^{336SCM}, which do not inhibit LtxA binding to cholesterol, had minimal effect on LtxA-mediated cell death (% cytotoxicity = 0.97 and 0.98, respectively). CRAC^{503WT}, which only slightly inhibited LtxA binding to cholesterol, had no effect on LtxA-mediated cell death (% cytotoxicity = 1.03). The ability of each peptide to inhibit binding to cholesterol by LtxA correlates with its inhibition of LtxA-mediated cytotoxicity, indicating that binding to cholesterol by the toxin is a required step in its cytolysis.

CRAC^{336} Is Required for LtxA to Kill Target Cells—To confirm the *in vitro* binding studies that utilized CRAC peptides, point mutations were induced in *ltx*A CRAC^{336} and CRAC^{503} sites to determine whether cholesterol binding affected LtxA-mediated cytolysis *in vivo*. Using site-directed mutagenesis, proline was substituted for tyrosine at amino acid positions 336 (for CRAC^{336}) or 503 (for CRAC^{503}) of individual *ltx*A. LtxA^{WT} and *ltx*A with the CRAC mutant genes were cloned into pSHH and expressed in tandem with *ltx*C under the control of the wild type leukotoxin promoter. Overnight cultures of LtxA and

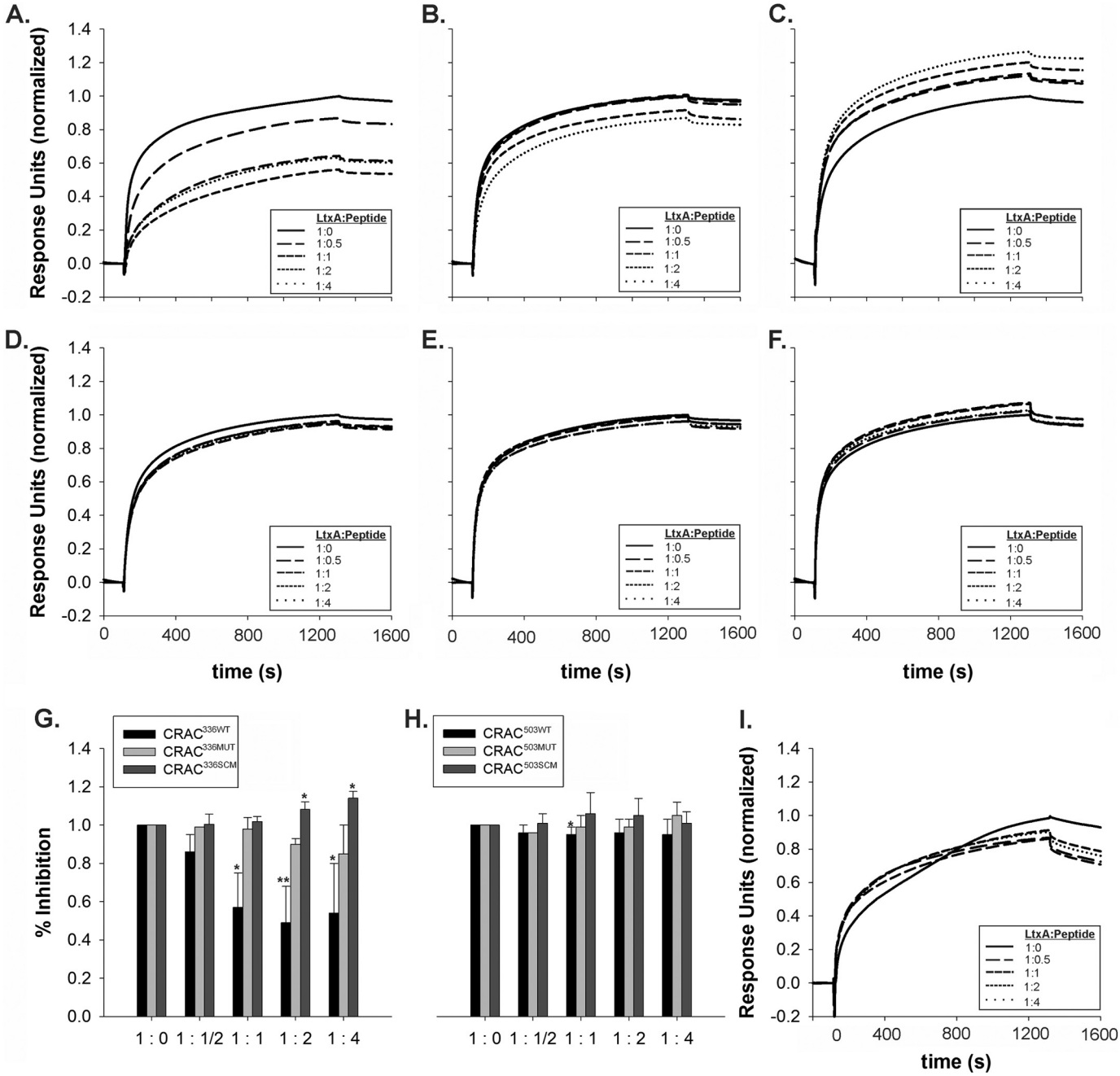

FIGURE 7. **Inhibition of LtxA^{wt} binding to cholesterol-containing membranes by CRAC 1 and CRAC 2 peptides.** *A*, CRAC^{336WT} at ratios of 1:0, 1:0.5, 1:1, 1:2, and 1:4 inhibits binding of LtxA^{wt} to membranes containing 40% cholesterol. *B* and *C*, however, CRAC^{336MUT} (*B*) and CRAC^{336SCM} (*C*) at ratios of 1:0 1:0.5, 1:1, 1:2, and 1:4 do not inhibit binding of LtxA^{wt} to membranes containing 40% cholesterol. *D*, CRAC^{503WT} at ratios of 1:0, 1:0.5, 1:1, 1:2, and 1:4 does not inhibit binding of LtxA^{wt} to membranes containing 40% cholesterol. *E* and *F*, likewise, CRAC^{503MUT} (*E*) and CRAC^{503SCM} (*F*) at ratios of 1:0, 1:0.5, 1:1, 1:2, and 1:4 do not inhibit binding of LtxA^{wt} to membranes containing 40% cholesterol. *G*, the CRAC^{336WT} peptide inhibits LtxA^{wt} binding to membranes containing 40% cholesterol (*black bars*), but disruption of the CRAC site by changing Tyr to Pro (*light gray bars*, CRAC^{336MUT}) or by scrambling the CRAC site (*dark gray bars*, CRAC^{336SCM}) prevents inhibition. *H*, the CRAC^{503} peptides (CRAC^{503WT}, CRAC^{503MUT}, and CRAC^{503SCM}) do not inhibit LtxA^{wt} binding to membranes containing 40% cholesterol. *I*, CRAC^{336WT} at ratios of 1:0, 1:0.5, 1:1, 1:2, and 1:4 only slightly inhibits binding of LtxA^{wt} to liposomes that do not contain cholesterol. The data represent the averages of three experiments, and the *error bars* represent the standard deviation. **, $p < 0.01$; *, $p < 0.05$.

LtxA-CRAC mutants were constitutively expressed in the *E. coli* DH5α cytosol and stained with rabbit anti-LtxA antibody (Fig. 8, insert). Following sonication, supernatants from each experimental group and controls were normalized for protein content and incubated with Jn.9 target cells. The cytotoxicity was measured with a trypan blue cytotoxicity assay (32).

Jn.9 cells exposed to LtxA^{WT} sonicates expressed in *E. coli* had a reduced viability after 24 h of exposure (41.0 ± 15.0%), when compared with a control sonicate that did not contain *ltx*A (94.4 ± 0.5%, $p < 0.001$). Cells exposed to the CRAC^{Y503P} mutant had a viability (49.7 ± 19.3%, $p = 0.02$) that was only slightly higher than cells exposed to wild type toxin. However, the CRAC^{Y336P} mutant was incapable of killing Jn.9 target cells (87.7 ± 3.3%, $p = 0.04$). These results indicate that an intact CRAC^{336} site is required for LtxA toxicity, whereas the CRAC^{503} site plays only a limited role in toxicity.

TABLE 8

Inhibition of LtxA-mediated cytotoxicity by CRAC peptides

LtxA was preincubated with the CRAC peptides at a molar ratio of 1:2 before being incubated with Jn.9 cells.

Toxin	Peptide mutation	Cytotoxicity[a]
		% untreated control
None		0.00
LtxA		1.00
LtxA + $CRAC^{336WT}$	None	0.06 ± 0.10
LtxA + $CRAC^{336MUT}$	Tyr → Pro	0.97 ± 0.43
LtxA + $CRAC^{336SCM}$	Scrambled	0.98 ± 0.37
LtxA + $CRAC^{503WT}$	None	1.03 ± 0.28
$CRAC^{336WT}$ alone	None	0.19 ± 0.38
$CRAC^{336MUT}$ alone	Tyr → Pro	0.34 ± 0.25
$CRAC^{336SCM}$ alone	Scrambled	0.28 ± 0.36
$CRAC^{503WT}$ alone	None	0.00 ± 0.56

[a] Cytotoxicity was measured using a trypan blue assay (32). The number of cells killed under each experimental condition was normalized to the number of cells killed by LtxA alone (after 5 h). Cytotoxicity was calculated as the number of cells killed relative to an untreated control. Each value represents the mean of three experiments ± standard deviation.

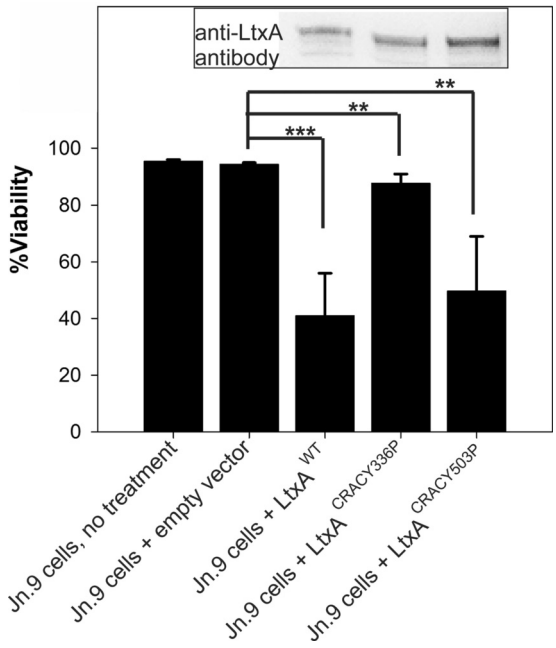

FIGURE 8. **Mutation of $CRAC^{336}$ affects LtxA cytotoxicity.** Point mutations were induced in *ltx*A by substituting proline for tyrosine at amino acid positions 336 (for $CRAC^{336}$) and 503 (for $CRAC^{503}$), using site-directed mutagenesis. LtxA wild type and CRAC mutant genes were cloned into pSHH and expressed in tandem with *ltx*C under the control of the native leukotoxin promoter. The *inset* shows a Western blot of the cytosolic fractions of wild type and CRAC mutants stained with anti-LtxA antibody. Overnight cultures of LtxA and LtxA CRAC mutants were constitutively expressed in the *E. coli* DH5α cytosol. Jn.9 cells were treated with 50 μg of total protein from the *E. coli* cytosolic fractions for 24 h. Jn.9 cells exposed to $LtxA^{WT}$ sonicates expressed in *E. coli* had a reduced viability after 24 h of exposure (41.0 ± 15.0%) when compared with a control sonicate that did not contain *ltx*A (94.4 ± 0.5%, $p < 0.001$). A point mutation in *ltx*A that replaced Tyr^{336} with Pro^{336} ($CRAC^{Y336P}$) yielded a toxin mutant incapable of killing target cells (87.7 ± 3.3%, $p = 0.04$). On the other hand, whereas *in vitro* studies had demonstrated the ability of $CRAC^{503}$ to bind cholesterol, cells exposed to the $CRAC^{Y503P}$ mutant had a viability (49.7 ± 19.3%, $p = 0.02$) that was only slightly higher than in cells exposed to wild type toxin. A sonicate from *E. coli* DH5α containing the pSHH empty vector served as the negative control. Cell death was measured with a trypan blue assay using a Vi-cell machine. ***, $p < 0.001$; **, $p < 0.05$, relative to the empty vector control.

DISCUSSION

LtxA-induced raft clustering is dependent upon a toxin-induced increase in cytosolic Ca^{2+}, activation of calpain, and cleavage of talin, which allows mobilization to and subsequent clustering of LtxA and its receptor, LFA-1, in lipid rafts (14). Furthermore, other RTX toxins, such as a leukotoxin (Lkt) produced by *M. hemolytica* and the adenylate cyclase toxin (CyaA) produced by *B. pertussis*, have been shown to have similar effects on raft and receptor clustering (16, 47). Here, we describe a unique mechanism of cholesterol binding by LtxA, which we hypothesize to be involved in this previously reported RTX/receptor clustering in lipid rafts.

Cholesterol-rich lipid rafts are dynamic and complex structures that admit or exclude certain proteins; as such, they provide platforms for signaling cascades (48). For example, LFA-1 clustering in lipid rafts plays several important roles in the ontogeny of immune responses, such as the formation of an immunological synapse (49, 50) or the arrest of immune cells on endothelia expressing intercellular adhesion molecules (51). In addition, cholesterol-rich lipid rafts play central roles in the pathogenesis of various microorganisms in many different ways, including docking, internalization, hiding, hijacking cell signaling, and oligomerization (52–59). FimH-expressing *E. coli* binds to the glycosylphosphatidylinositol-linked protein CD48, which is located in lipid rafts, as a first step in internalization (56). Bacteria, including *Campylobacter jejuni* and *Mycobacterium bovis*, as well as viruses are internalized in raft-dependent processes (53–55, 58). A number of bacterial toxins, including streptolysin O, *Vibrio cholerae* cytolysin, and anthrax toxin, have been shown to use lipid rafts as a concentrating platform for oligomerization (52, 59), whereas thiol-activated/thiol-dependent streptolysins and listerolysin use raft lipids as receptors (57).

The mechanism of lipid raft association and cholesterol binding by LtxA appears to be distinct from these previously reported mechanisms. We have shown that LtxA binds specifically to cholesterol-containing membranes in a unique mechanism with a strong cholesterol-dependent dissociation rate but a cholesterol-independent association rate (Fig. 2). Two regions of the deduced amino acid sequence of LtxA, ^{334}LEEYSKR^{339} ($CRAC^{336}$) and ^{502}VDYLKK^{505} ($CRAC^{503}$), were identified as potential cholesterol binding sites, based upon the CRAC motif, (L/V)X_{1-5}YX_{1-5}(R/K) (60, 61). Although both sites are juxtaposed to the LtxA hydrophobic domain, the requirements for a CRAC motif are quite flexible, and therefore, not all predicted CRAC sites bind cholesterol or possess an *in vivo* function. For this reason, we undertook an experimental approach employing SPR and DSC with LtxA and synthetic peptides corresponding to both $CRAC^{336}$ and $CRAC^{503}$ (Table 5). Our results indicate that LtxA binds cholesterol strongly, and both CRAC peptides $CRAC^{336WT}$ and $CRAC^{503WT}$ also interact strongly with cholesterol. However, only $CRAC^{336WT}$ was able to inhibit binding of LtxA to cholesterol. $CRAC^{503WT}$ and all of the control peptides had no effect on binding of LtxA to cholesterol. In addition, only $CRAC^{336WT}$, the only peptide to inhibit binding to cholesterol, inhibited LtxA-mediated cytotoxicity. This behavior is consistent with our previous work, in which we found that extraction of cholesterol from Jn.9 cells inhibits LtxA-mediated cytotoxicity (14). In the panel of CRAC mutants, modification of $CRAC^{336}$ reduced the cytotoxicity of LtxA, whereas modification of $CRAC^{503}$ had only a limited effect on the cytotoxicity of LtxA.

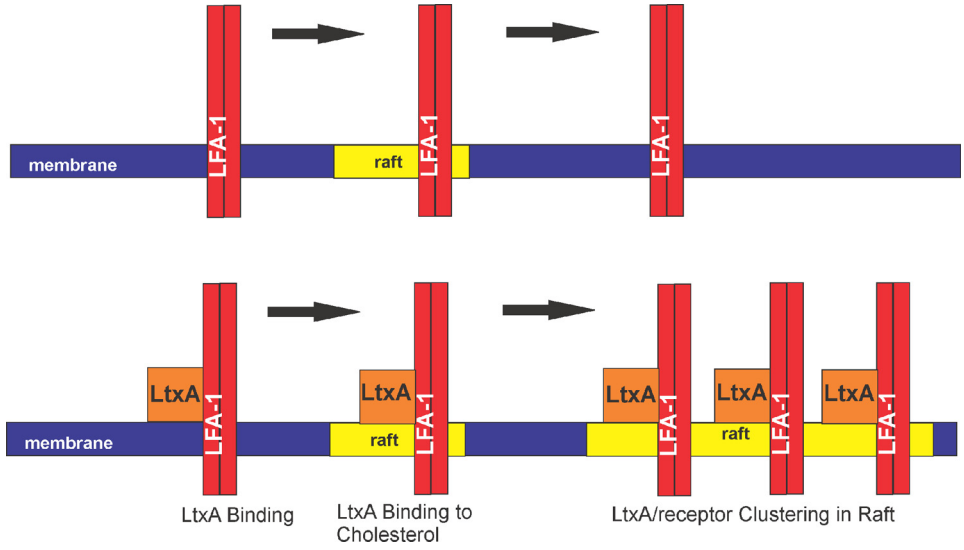

FIGURE 9. **Proposed mechanism of LtxA binding and resulting LFA-1/LtxA clustering in lipid rafts.** In the absence of LtxA, LFA-1 moves transiently into and out of lipid rafts (*top panel*). Binding of cholesterol by LtxA is almost irreversible, and therefore, transient movement of the LtxA·LFA-1 complex into the raft becomes "permanent," resulting in large LtxA·LFA-1 clusters in the lipid rafts (*bottom panel*).

Together, the results indicate that although both CRAC sites may interact with cholesterol, the first CRAC site, $CRAC^{336}$, is responsible for cholesterol binding by LtxA. Interestingly, this first CRAC site is highly conserved among RTX toxins, indicating that this mechanism may be common to other members of this toxin family (Table 4). The second CRAC site, $CRAC^{503}$, which appears to have a less important role in cholesterol binding and cytotoxicity of LtxA, is less conserved among the RTX toxins, appearing only in LtxA.

Our data indicate that cholesterol binding by LtxA is mediated by $CRAC^{336}$; however, we could not rule out the possibility that the acyl groups attached to LtxA could also be involved in the process. For some proteins, acylation is required for membrane binding (62–66); however, the role of acylation in the RTX toxins has not yet been conclusively determined (34). Studies have shown that acylation does not affect the ability of *E. coli* α-HlyA to bind to either erythrocytes or liposomes (67, 68), but others have shown that acylation is involved in this process (69–71). Alternatively, acylation of the RTX toxins has been proposed to be involved in protein-protein interactions or pore formation (34, 68, 69, 72). Previously, we showed that the acyl chains on LtxA are saturated and/or hydroxylated (10); this hydroxylation may sterically inhibit association with cholesterol-containing membranes, which are more tightly packed than cholesterol-poor membranes. Acylation clearly plays a role in cytotoxicity, because the nonacylated mutant was unable to kill Jn.9 cells (Table 1); however, it appears that the role of acylation in the cytotoxic mechanism is not the binding to cholesterol, because there was no significant difference in the binding of acylated LtxA ($LtxA^{ltxC/+ltxC}$) to cholesterol compared with unacylated LtxA ($LtxA^{ltxC}$).

LtxA is not the only toxin produced by *A. actinomycetemcomitans* that binds to cholesterol using CRAC sequences. The cytolethal distending toxin produced by this organism binds membrane cholesterol before gaining access to the cytoplasm, where it triggers cell cycle arrest (43). Surprisingly, although both the *A. actinomycetemcomitans*-produced cytolethal distending toxin and LtxA bind cholesterol via CRAC sites, the mechanisms of binding of the toxins are quite different. The affinity of the cytolethal distending toxin for cholesterol occurs through an increased association rate when binding to cholesterol and cholesterol-rich rafts (43), suggesting that the cytolethal distending toxin uses cholesterol as a receptor. Conversely, the affinity of LtxA for cholesterol is not dependent upon differences in association rate (k_a); rather, it is influenced by the cholesterol-dependent change in dissociation rate (k_d), suggesting that LtxA is more indiscriminate in its binding, but once bound to cholesterol, the attachment is almost irreversible.

The lipid compositions used in this work were specifically chosen for their raft-forming nature. At room temperature, a membrane composed of DMPC and 0% cholesterol exists in a non-raft-like (liquid-disordered) phase, whereas at 40 and 60% cholesterol, the membrane exists in a raft-like (liquid-ordered phase) (27, 28). *In vitro*, the lipid composition of lipid rafts is often ~30% (74–77). The cholesterol compositions used in this work are valid in both an *in vitro* and *in vivo* context.

Previous work in our lab found that LtxA is located in lipid rafts only after it has bound to its receptor, LFA-1. Before the binding of LtxA, LFA-1 is located outside of the raft, and upon LtxA binding, the LtxA·LFA-1 complex moves to the raft, causing large scale clustering (14). Here, we demonstrated that the association rate of LtxA to membranes does not change with the cholesterol composition; in other words, LtxA does not have a clear preference for binding to cholesterol, an observation that is consistent with this previous paper, in which LtxA was found in both raft (cholesterol-rich) and non-raft (cholesterol-poor) regions of the membrane. Once LtxA binds to cholesterol, however, it remains tightly bound, providing a possible mechanism for the observed LtxA·LFA-1 clustering in lipid rafts (Fig. 9). Movement of proteins in and out of rafts is often transient (23, 33, 46), and LFA-1 has been shown to reside in two subsets: one within rafts and one outside (73). We hypothesize that LFA-1 is able to move into and out of rafts until it is bound by LtxA, at which point, LtxA binds tightly to choles-

terol, holding the LtxA·LFA-1 complex in the raft and allowing the formation of large clusters within the raft. Because we have found that binding of LtxA to cholesterol is essential for LtxA-mediated cell death, we propose that this cholesterol-dependent clustering is a key step in the cytotoxicity of LtxA.

The specific binding of other RTX toxins to cholesterol has not been reported previously, although it has been shown that both CyaA and Lkt cause a receptor/toxin clustering in lipid rafts (16, 47). The mechanism of raft clustering by Lkt is similar to what we have reported for LtxA; here, we have shown that Lkt shares $CRAC^{336}$ with LtxA, suggesting that the binding of cholesterol by this RTX toxin may drive this receptor-dependent clustering in lipid rafts. However, CyaA, which does not contain either of the two CRAC sites, has been shown to induce the clustering of $\alpha_M\beta_2$ integrins in lipid rafts (47). The mechanism by which CyaA clusters in rafts differs slightly from the mechanism used by LtxA (47); an interesting question will be whether this difference in mechanism can be explained by the lack of a CRAC site in CyaA or the fact that CyaA binds to a different β2 integrin than does LtxA.

In this work, we have identified a unique but likely conserved mechanism of cholesterol binding by a bacterial toxin. The binding of cholesterol by LtxA occurs in an indirect fashion but appears to regulate the cholesterol dependence of LtxA cytotoxicity.

Acknowledgments—We thank Patrik Nygren and Tina Cairns for technical expertise in SPR and Ellis Golub for help with sequence alignment.

REFERENCES

1. Taichman, N. S., Simpson, D. L., Sakurada, S., Cranfield, M., DiRienzo, J., and Slots, J. (1987) Comparative studies on the biology of *Actinobacillus actinomycetemcomitans* leukotoxin in primates. *Oral Microbiol. Immunol.* **2,** 97–104
2. Isberg, R. R., and Tran Van Nhieu, G. (1994) Binding and internalization of microorganisms by integrin receptors. *Trends Microbiol.* **2,** 10–14
3. Welch, R. A. (1991) Pore-forming cytolysins of gram-negative bacteria. *Mol. Microbiol.* **5,** 521–528
4. Lally, E. T., Kieba, I. R., Sato, A., Green, C. L., Rosenbloom, J., Korostoff, J., Wang, J. F., Shenker, B. J., Ortlepp, S., Robinson, M. K., and Billings, P. C. (1997) RTX toxins recognize a β2 integrin on the surface of human target cells. *J. Biol. Chem.* **272,** 30463–30469
5. Guermonprez, P., Khelef, N., Blouin, E., Rieu, P., Ricciardi-Castagnoli, P., Guiso, N., Ladant, D., and Leclerc, C. (2001) The adenylate cyclase toxin of *Bordetella pertussis* binds to target cells via the $\alpha_M\beta_2$ integrin (CD11b/CD18). *J. Exp. Med.* **193,** 1035–1044
6. Crosby, J. A., and Kachlany, S. C. (2007) TdeA, a TolC-like protein required for toxin and drug export in *Aggregatibacter* (*Actinobacillus*) *actinomycetemcomitans*. *Gene* **388,** 83–92
7. Hackett, M., Guo, L., Shabanowitz, J., Hunt, D. F., and Hewlett, E. L. (1994) Internal lysine palmitoylation in adenylate cyclase toxin from *Bordetella pertussis*. *Science* **266,** 433–435
8. Hardie, K. R., Issartel, J. P., Koronakis, E., Hughes, C., and Koronakis, V. (1991) *In vitro* activation of *Escherichia coli* prohaemolysin to the mature membrane-targeted toxin requires HlyC and a low molecular-weight cytosolic polypeptide. *Mol. Microbiol.* **5,** 1669–1679
9. Issartel, J. P., Koronakis, V., and Hughes, C. (1991) Activation of *Escherichia coli* prohaemolysin to the mature toxin by acyl carrier protein-dependent fatty acylation. *Nature* **351,** 759–761
10. Fong, K. P., Tang, H. Y., Brown, A. C., Kieba, I. R., Speicher, D. W., Boesze-Battaglia, K., and Lally, E. T. (2011) *Aggregatibacter actinomycetemcomitans* leukotoxin is post-translationally modified by addition of either saturated or hydroxylated fatty acyl chains. *Mol. Oral Microbiol.* **26,** 262–276
11. Bakás, L., Ostolaza, H., Vaz, W. L., and Goñi, F. M. (1996) Reversible adsorption and nonreversible insertion of *Escherichia coli* α-hemolysin into lipid bilayers. *Biophys. J.* **71,** 1869–1876
12. Lear, J. D., Karakelian, D., Furblur, U., Lally, E. T., and Tanaka, J. C. (2000) Conformational studies of *Actinobacillus actinomycetemcomitans* leukotoxin. Partial denaturation enhances toxicity. *Biochim. Biophys. Acta* **1476,** 350–362
13. Walters, M. J., Brown, A. C., Edrington, T. C., Baranwal, S., Du, Y., Lally, E. T., and Boesze-Battaglia, K. (2013) Membrane association and destabilization by *Aggregatibacter actinomycetemcomitans* leukotoxin requires changes in secondary structures. *Mol. Oral Microbiol.*, in press
14. Fong, K. P., Pacheco, C. M., Otis, L. L., Baranwal, S., Kieba, I. R., Harrison, G., Hersh, E. V., Boesze-Battaglia, K., and Lally, E. T. (2006) *Actinobacillus actinomycetemcomitans* leukotoxin requires lipid microdomains for target cell cytotoxicity. *Cell Microbiol.* **8,** 1753–1767
15. Bumba, L., Masin, J., Fiser, R., and Sebo, P. (2010) *Bordetella* adenylate cyclase toxin mobilizes its β2 integrin receptor into lipid rafts to accomplish translocation across target cell membrane in two steps. *PLoS. Pathog.* **6,** e1000901
16. Atapattu, D. N., and Czuprynski, C. J. (2007) *Mannheimia haemolytica* leukotoxin binds to lipid rafts in bovine lymphoblastoid cells and is internalized in a dynamin-2- and clathrin-dependent manner. *Infect. Immun.* **75,** 4719–4727
17. Carman, C. V., and Springer, T. A. (2003) Integrin avidity regulation. Are changes in affinity and conformation underemphasized? *Curr. Opin. Cell Biol.* **15,** 547–556
18. Balashova, N. V., Shah, C., Patel, J. K., Megalla, S., and Kachlany, S. C. (2009) *Aggregatibacter actinomycetemcomitans* LtxC is required for leukotoxin activity and initial interaction between toxin and host cells. *Gene* **443,** 42–47
19. Fine, D. H., Furgang, D., Schreiner, H. C., Goncharoff, P., Charlesworth, J., Ghazwan, G., Fitzgerald-Bocarsly, P., and Figurski, D. H. (1999) Phenotypic variation in *Actinobacillus actinomycetemcomitans* during laboratory growth. Implications for virulence. *Microbiology* **145,** 1335–1347
20. Kachlany, S. C., Fine, D. H., and Figurski, D. H. (2002) Purification of secreted leukotoxin (LtxA) from *Actinobacillus actinomycetemcomitans*. *Protein Expr. Purif.* **25,** 465–471
21. Lally, E. T., Golub, E. E., Kieba, I. R., Taichman, N. S., Decker, S., Berthold, P., Gibson, C. W., Demuth, D. R., and Rosenbloom, J. (1991) Structure and function of the B and D genes of the *Actinobacillus actinomycetemcomitans* leukotoxin complex. *Microb. Pathog.* **11,** 111–121
22. Cherry, L. K., Weber, K. S., and Klickstein, L. B. (2001) A dominant Jurkat T cell mutation that inhibits LFA-1-mediated cell adhesion is associated with increased cell growth. *J. Immunol.* **167,** 6171–6179
23. Edidin, M. (2003) The state of lipid rafts. From model membranes to cells. *Annu. Rev. Biophys. Biomol. Struct.* **32,** 257–283
24. Hope, M. J., Bally, M. B., Webb, G., and Cullis, P. R. (1985) Production of large unilamellar vesicles by a rapid extrusion procedure: characterization of size distribution, trapped volume and ability to maintain a membrane potential. *Biochim. Biophys. Acta* **812,** 55–65
25. MacDonald, R. C., MacDonald, R. I., Menco, B. P., Takeshita, K., Subbarao, N. K., and Hu, L. R. (1991) Small-volume extrusion apparatus for preparation of large, unilamellar vesicles. *Biochim. Biophys. Acta* **1061,** 297–303
26. Dietrich, C., Bagatolli, L. A., Volovyk, Z. N., Thompson, N. L., Levi, M., Jacobson, K., and Gratton, E. (2001) Lipid rafts reconstituted in model membranes. *Biophys. J.* **80,** 1417–1428
27. Brown, A. C., Towles, K. B., and Wrenn, S. P. (2007) Measuring raft size as a function of membrane composition in PC-based systems. Part 1: Binary systems. *Langmuir* **23,** 11180–11187
28. Almeida, P. F., Vaz, W. L., and Thompson, T. E. (1992) Lateral diffusion in the liquid phases of dimyristoylphosphatidylcholine/cholesterol lipid bilayers. A free volume analysis. *Biochemistry* **31,** 6739–6747
29. Deleted in proof
30. Besenicar, M. P., and Anderluh, G. (2010) Preparation of lipid membrane surfaces for molecular interaction studies by surface plasmon resonance biosensors. *Methods Mol. Biol.* **627,** 191–200

31. Brown, A. C., Boesze-Battaglia, K., Du, Y., Stefano, F. P., Kieba, I. R., Epand, R. F., Kakalis, L., Yeagle, P. L., Epand, R. M., and Lally, E. T. (2012) *Aggregatibacter actinomycetemcomitans* leukotoxin cytotoxicity occurs through bilayer destabilization. *Cell. Microbiol.* **14,** 869–881
32. Brogan, J. M., Lally, E. T., Poulsen, K., Kilian, M., and Demuth, D. R. (1994) Regulation of *Actinobacillus actinomycetemcomitans* leukotoxin expression. Analysis of the promoter regions of leukotoxic and minimally leukotoxic strains. *Infect. Immun.* **62,** 501–508
33. Bini, L., Pacini, S., Liberatori, S., Valensin, S., Pellegrini, M., Raggiaschi, R., Pallini, V., and Baldari, C. T. (2003) Extensive temporally regulated reorganization of the lipid raft proteome following T-cell antigen receptor triggering. *Biochem. J.* **369,** 301–309
34. Stanley, P., Koronakis, V., and Hughes, C. (1998) Acylation of *Escherichia coli* hemolysin. A unique protein lipidation mechanism underlying toxin function. *Microbiol. Mol. Biol. Rev.* **62,** 309–333
35. Kyte, J., and Doolittle, R. F. (1982) A simple method for displaying the hydropathic character of a protein. *J. Mol. Biol.* **157,** 105–132
36. Lally, E. T., Golub, E. E., Kieba, I. R., Taichman, N. S., Rosenbloom, J., Rosenbloom, J. C., Gibson, C. W., and Demuth, D. R. (1989) Analysis of the *Actinobacillus actinomycetemcomitans* leukotoxin gene. Delineation of unique features and comparison to homologous toxins. *J. Biol. Chem.* **264,** 15451–15456
37. Chou, P. Y., and Fasman, G. D. (1978) Empirical predictions of protein conformation. *Annu. Rev. Biochem.* **47,** 251–276
38. Chou, P. Y., and Fasman, G. D. (1978) Prediction of the secondary structure of proteins from their amino acid sequence. *Adv. Enzymol. Relat Areas Mol. Biol.* **47,** 45–148
39. Baumann, U., Wu, S., Flaherty, K. M., and McKay, D. B. (1993) Three-dimensional structure of the alkaline protease of *Pseudomonas aeruginosa*. A two-domain protein with a calcium binding parallel β roll motif. *EMBO J.* **12,** 3357–3364
40. Lilie, H., Haehnel, W., Rudolph, R., and Baumann, U. (2000) Folding of a synthetic parallel β-roll protein. *FEBS Lett.* **470,** 173–177
41. Lally, E. T., Kieba, I. R., Taichman, N. S., Rosenbloom, J., Gibson, C. W., Demuth, D. R., Harrison, G., and Golub, E. E. (1991) *Actinobacillus actinomycetemcomitans* leukotoxin is a calcium-binding protein. *J. Periodontal Res.* **26,** 268–271
42. Jarchau, T., Chakraborty, T., Garcia, F., and Goebel, W. (1994) Selection for transport competence of C-terminal polypeptides derived from *Escherichia coli* hemolysin. The shortest peptide capable of autonomous HlyB/HlyD-dependent secretion comprises the C-terminal 62 amino acids of HlyA. *Mol. Gen. Genet.* **245,** 53–60
43. Boesze-Battaglia, K., Brown, A., Walker, L., Besack, D., Zekavat, A., Wrenn, S., Krummenacher, C., and Shenker, B. J. (2009) Cytolethal distending toxin-induced cell cycle arrest of lymphocytes is dependent upon recognition and binding to cholesterol. *J. Biol. Chem.* **284,** 10650–10658
44. Jamin, N., Neumann, J. M., Ostuni, M. A., Vu, T. K., Yao, Z. X., Murail, S., Robert, J. C., Giatzakis, C., Papadopoulos, V., and Lacapère, J. J. (2005) Characterization of the cholesterol recognition amino acid consensus sequence of the peripheral-type benzodiazepine receptor. *Mol. Endocrinol.* **19,** 588–594
45. Epand, R. M., Bach, D., Borochov, N., and Wachtel E. (2000) Cholesterol crystalline polymorphism and the solubility of cholesterol in phosphatidylserine. *Biophys. J.* **78,** 866–873
46. Hancock, J. F. (2006) Lipid rafts. Contentious only from simplistic standpoints. *Nat. Rev. Mol. Cell Biol.* **7,** 456–462
47. Bumba, L., Masin, J., Fiser, R., and Sebo, P. (2010) *Bordetella* adenylate cyclase toxin mobilizes its beta2 integrin receptor into lipid rafts to accomplish translocation across target cell membrane in two steps. *PLoS Pathog.* **6,** e1000901
48. Simons, K., and Toomre, D. (2000) Lipid rafts and signal transduction. *Nat. Rev. Mol. Cell Biol.* **1,** 31–39
49. Grakoui, A., Bromley, S. K., Sumen, C., Davis, M. M., Shaw, A. S., Allen, P. M., and Dustin, M. L. (1999) The immunological synapse. A molecular machine controlling T cell activation. *Science* **285,** 221–227
50. Monks, C. R., Freiberg, B. A., Kupfer, H., Sciaky, N., and Kupfer, A. (1998) Three-dimensional segregation of supramolecular activation clusters in T cells. *Nature* **395,** 82–86
51. Stewart, M. P., McDowall, A., and Hogg, N. (1998) LFA-1-mediated adhesion is regulated by cytoskeletal restraint and by a Ca^{2+}-dependent protease, calpain. *J. Cell Biol.* **140,** 699–707
52. Abrami, L., Liu, S., Cosson, P., Leppla, S. H., and van der Goot, F. G. (2003) Anthrax toxin triggers endocytosis of its receptor via a lipid raft-mediated clathrin-dependent process. *J. Cell Biol.* **160,** 321–328
53. Ahn, A., Gibbons, D. L., and Kielian, M. (2002) The fusion peptide of Semliki Forest virus associates with sterol-rich membrane domains. *J. Virol.* **76,** 3267–3275
54. Gatfield, J., and Pieters, J. (2000) Essential role for cholesterol in entry of mycobacteria into macrophages. *Science* **288,** 1647–1650
55. Norkin, L. C. (1999) Simian virus 40 infection via MHC class I molecules and caveolae. *Immunol. Rev.* **168,** 13–22
56. Shin, J.-S., Gao, Z., and Abraham, S. N. (2000) Involvement of cellular caveolae in bacterial entry into mast cells. *Science* **289,** 785–788
57. Tweten, R. K. (2005) Cholesterol-dependent cytolysins, a family of versatile pore-forming toxins. *Infect. Immun.* **73,** 6199–6209
58. Wooldridge, K. G., Williams, P. H., and Ketley, J. M. (1996) Host signal transduction and endocytosis of *Campylobacter jejuni*. *Microb. Pathog.* **21,** 299–305
59. Zitzer, A., Bittman, R., Verbicky, C. A., Erukulla, R. K., Bhakdi, S., Weis, S., Valeva, A., and Palmer, M. (2001) Coupling of cholesterol and cone-shaped lipids in bilayers augments membrane permeabilization by the cholesterol-specific toxins streptolysin O and *Vibrio cholerae* cytolysin. *J. Biol. Chem.* **276,** 14628–14633
60. Li, H., and Papadopoulos, V. (1998) Peripheral-type benzodiazepine receptor function in cholesterol transport. Identification of a putative cholesterol recognition/interaction amino acid sequence and consensus pattern. *Endocrinology* **139,** 4991–4997
61. Li, H., Yao, Z., Degenhardt, B., Teper, G., and Papadopoulos, V. (2001) Cholesterol binding at the cholesterol recognition/ interaction amino acid consensus (CRAC) of the peripheral-type benzodiazepine receptor and inhibition of steroidogenesis by an HIV TAT-CRAC peptide. *Proc. Natl. Acad. Sci. U.S.A.* **98,** 1267–1272
62. Buss, J. E., Kamps, M. P., Gould, K., and Sefton, B. M. (1986) The absence of myristic acid decreases membrane binding of p60src but does not affect tyrosine protein kinase activity. *J. Virol.* **58,** 468–474
63. Resh, M. D. (2006) Trafficking and signaling by fatty-acylated and prenylated proteins. *Nature Chemical Biology* **2,** 584–590
64. Bryant, M., and Ratner, L. (1990) Myristoylation-dependent replication and assembly of human immunodeficiency virus 1. *Proc. Natl. Acad. Sci. U.S.A.* **87,** 523–527
65. Schultz, A. M., and Rein, A. (1989) Unmyristylated Moloney murine leukemia virus Pr65gag is excluded from virus assembly and maturation events. *J. Virol.* **63,** 2370–2373
66. Weaver, T. A., and Panganiban, A. T. (1990) *N*-Myristoylation of the spleen necrosis virus matrix protein is required for correct association of the Gag polyprotein with intracellular membranes and for particle formation. *J. Virol.* **64,** 3995–4001
67. Bauer, M. E., and Welch, R. A. (1996) Association of RTX toxins with erythrocytes. *Infect. Immun.* **64,** 4665–4672
68. Soloaga, A., Ostolaza, H., Goñi, F. M., and de la Cruz, F. (1996) Purification of *Escherichia coli* pro-haemolysin, and a comparison with the properties of mature α-haemolysin. *Eur. J. Biochem.* **238,** 418–422
69. Herlax, V., and Bakás, L. (2003) Acyl chains are responsible for the irreversibility in the *Escherichia coli* α-hemolysin binding to membranes. *Chem. Phys. Lipids* **122,** 185–190
70. Hackett, M., Walker, C. B., Guo, L., Gray, M. C., Van Cuyk, S., Ullmann, A., Shabanowitz, J., Hunt, D. F., Hewlett, E. L., and Sebo, P. (1995) Hemolytic, but not cell-invasive activity, of adenylate cyclase toxin is selectively affected by differential fatty-acylation in *Escherichia coli*. *J. Biol. Chem.* **270,** 20250–20253
71. Boehm, D. F., Welch, R. A., and Snyder, I. S. (1990) Domains of *Escherichia coli* hemolysin (HlyA) involved in binding of calcium and erythrocyte membranes. *Infect. Immun.* **58,** 1959–1964
72. Boyd, A. P., Ross, P. J., Conroy, H., Mahon, N., Lavelle, E. C., and Mills, K. H. (2005) *Bordetella pertussis* adenylate cyclase toxin modulates innate and adaptive immune responses. Distinct roles for acylation and enzymatic activ-

ity in immunomodulation and cell death. *J. Immunol.* **175,** 730–738
73. Marwali, M. R., Rey-Ladino, J., Dreolini, L., Shaw, D., and Takei, F. (2003) Membrane cholesterol regulates LFA-1 function and lipid raft heterogeneity. *Blood* **102,** 215–222
74. Brown, D. A., and Rose, J. K. (1992) Sorting of GPI-anchored proteins to glycolipid-enriched membrane subdomains during transport to the apical cell surface. *Cell* **68,** 533–544
75. Schuck, S., Honsho, M., Ekroos, K., Shevchenko, A., and Simons, K. (2003) Resistance of cell membranes to different detergents. *Proc. Natl. Acad. Sci. U.S.A.* **100,** 5795–5800
76. Aloia, R. C., Tian, H., and Jensen, F. C. (1993) Lipid composition and fluidity of the human immunodeficiency virus envelope and host cell plasma membranes. *Proc. Natl. Acad. Sci. U.S.A.* **90,** 5181–5185
77. van Meer, G., Voelker, D. R., and Feigenson, G. W. (2008) Membrane lipids. Where they are and how they behave. *Nat. Rev. Mol. Cell Biol.* **9,** 112–124